Paper No.
11193

NACE INTERNATIONAL CORROSION 2018 Conference & Expo

Corrosion Inhibition of Carbon Steel in Supercritical CO_2/H_2S Environments

Yoon-Seok Choi, Shokrollah Hassani, Thanh Nam Vu, Srdjan Nesic
Institute for Corrosion and Multiphase Technology,
Department of Chemical and Biomolecular Engineering, Ohio University
342 West State Street
Athens, OH 45701
USA

Ahmad Zaki B Abas, Azmi Mohammed Nor, Muhammad Firdaus Suhor
Petronas Research SDN. BHD, Selangor Darul Ehsan, Malaysia

ABSTRACT

The effect of small amounts of H_2S on the corrosion behavior and corrosion protection of carbon steel was investigated in high pressure CO_2 environments. The experiments were carried out in a 7.5L autoclave with two combinations of CO_2 partial pressure and temperature (12 MPa/80°C and 8 MPa/25°C) with different H_2S concentrations (0, 100 and 200 ppm). The corrosion behavior of specimens was evaluated using electrochemical measurements and surface analytical techniques. It was found that the addition of small amounts of H_2S reduced the corrosion rate of carbon steel in high pressure CO_2 environments. However, the corrosion rate was still higher than the targeted rate (< 0.1 mm/y). Additional protection was required in order to achieve the target. Utilizing 400 ppm of an imidazoline-type corrosion inhibitor reduced the corrosion rate of carbon steel below 0.1 mm/y in a high pressure CO_2 condition with H_2S. Compared to carbon steel, the corrosion resistance of low Cr steels was lower in the corresponding CO_2 conditions with H_2S.

Key words: Supercritical/liquid CO_2, CO_2 corrosion, carbon steel, low Cr alloy steel, corrosion inhibitor

INTRODUCTION

Numerous studies of corrosion issues in high pressure CO_2 environments relating to carbon capture and storage (CCS), enhanced oil recovery (EOR), and deep water oil and gas production applications have recently been published.[1-5] Aqueous corrosion mechanisms in high pressure CO_2 are similar to those in low pressure CO_2 conditions.[6] However, the corrosion rate of carbon steel in the presence of high pressure CO_2 without formation of protective corrosion product layers is very high (≥ 20 mm/y) due to the presence of significantly high concentrations of corrosive species, such as H^+ and H_2CO_3.[7-14]

Controlling corrosion in such cases usually involves use of Corrosion Resistant Alloys (CRAs). Since the use of CRAs is very costly, there is a need to better quantify their performance, as well as that of mild steels, against the risk of corrosion associated with high pressure CO_2 environments. This facilitates identification of production conditions where mild steel may still be used in the construction of pipelines, and related, systems. Furthermore, this has the potential to significantly reduce costs associated with use of CRAs for infrastructure construction.

In previous studies, an attempt was made to control the corrosion of carbon steel in high pressure CO_2 conditions using low Cr alloy steels and corrosion inhibitor (CI).[15,16] The studies showed that utilizing low Cr alloy steels (1% Cr and 3% Cr) alone was insufficient to decrease the corrosion rate below the targeted value of 0.1 mm/y. Adequate protection was achieved by applying generic "imidazoline+thiosulfate" CI to carbon steel in the high pressure CO_2 environments. Furthermore, the CI performance with carbon steel was better than Cr-containing steels.

It has recently been reported that small amounts of H_2S can be present in high pressure CO_2 streams related to gas field development.[17,18] Although the effect of H_2S on the aqueous corrosion of carbon steel at low CO_2 partial pressures is well investigated, limited work has been done in high pressure CO_2 environments.[18-20] In addition, there is no systematic study on corrosion inhibition in high pressure CO_2 environments with H_2S. Thus, the objective of the present study was to identify and quantify the key issues that affect integrity of carbon steel in high pressure CO_2 in the presence of small amounts of H_2S, and to establish potential corrosion mitigation strategies using low Cr alloy steels and corrosion inhibitors.

EXPERIMENTAL PROCEDURE

The test specimens were machined from UNS K03014 carbon steel (CS), UNS G41300-1Cr steel (1Cr) and UNS G41300-3Cr steel (3Cr) with two different geometries: cylindrical type with 5 cm^2 exposed area for electrochemical measurements, and rectangular type with a size of 1.27 cm × 1.27 cm × 0.254 cm for surface analysis. The chemical compositions of the studied alloys are shown in Table 1. The specimens were ground sequentially with 250, 400 then 600-grit silicon carbide (SiC) paper, cleaned with isopropyl alcohol in an ultrasonic bath for 60 seconds, and dried. A 1 wt.% NaCl aqueous electrolyte was prepared using deionized (DI) water.

Table 1
Chemical compositions of materials used in the present study (wt.%, balance Fe).

	C	Cr	Mn	P	S	Si	Cu	Ni	Mo	Al
CS	0.065	0.05	1.54	0.013	0.001	0.25	0.04	0.04	0.007	0.041
1Cr	0.3	0.85	0.91	0.015	0.008	0.29	---	---	---	---
3Cr	0.08	3.43	0.54	0.006	0.003	0.3	0.16	0.06	0.32	---

An 'imidazoline + thiosulfate' generic corrosion inhibitor (CI1) and an 'imidazoline' generic corrosion inhibitor (CI2) were selected for evaluation under high pCO_2 environments with H_2S. In this instance, 'imidazoline' is shorthand for tall oil fatty acid (TOFA) imidazoline-type inhibitor.

The corrosion experiments were conducted in a 7.5-liter autoclave (UNS N10276) with a three-electrode setup, consisting of a working electrode, a high pressure/high temperature Ag/AgCl reference electrode and a platinum coated niobium counter electrode. An impeller was used to stir the solution at a rotation speed of 1000 rpm (corresponding to approximately 1 m/s), stirring was maintained during the test.

Experimental procedure is outlined in Figure 1. Initially, 1 wt.% of NaCl solution was placed in an autoclave and this electrolyte purged with CO_2 for 1 ~ 3 hours in order to remove dissolved O_2. The electrodes and specimens were then placed in the autoclave. After closing the autoclave, temperature was increased to the testing temperature. Once the working temperature was achieved, a mixture of CO_2 and H_2S was injected into the system to achieve the working H_2S partial pressure. High pressure CO_2 was then injected with a booster pump. Corrosion rate and corrosion potential of specimens were evaluated with time by linear polarization resistance (LPR) measurements. The details of LPR measurements are shown in our previous work.[16] After each test, the specimens were removed from the autoclave, rinsed with DI water and isopropyl alcohol, dried with N_2 and stored in a desiccator cabinet in an inert atmosphere until surface analyses could be conducted. For testing with inhibitors, the procedure was the same as shown in Figure 1, except inhibitor was added to the solution before inserting the specimens.

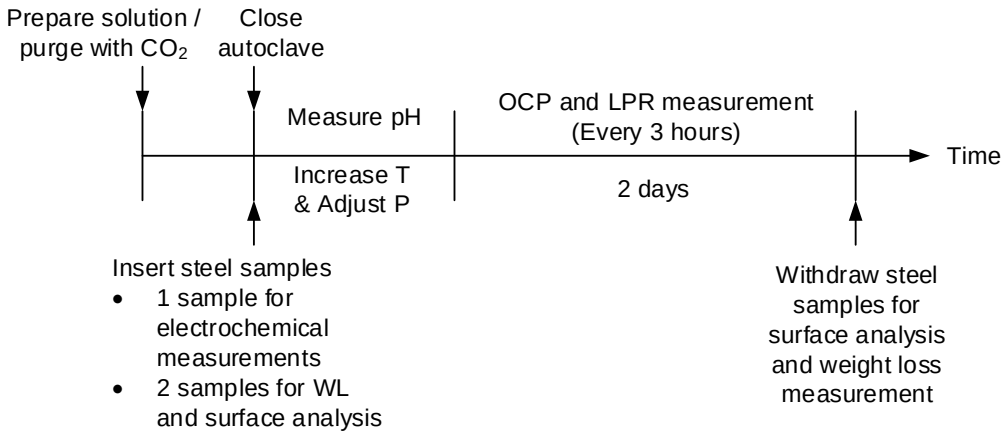

Figure 1: Experimental procedures for evaluating the corrosion behavior of materials in high pCO_2 environments with H_2S.

Table 2 shows the test conditions for the present study. The test conditions were set in order to simulate the inlet and outlet conditions for CO_2 transportation pipeline, where the CO_2 is present in a supercritical state at the 'inlet' condition and it exists as a liquid at the 'outlet' condition.[17]

Table 2
Test conditions for corrosion testing

	pCO_2 (MPa)	H_2S (ppm)	Temperature (^oC)
Inlet	12	0	80
	12	100	80
	12	200	80
Outlet	8	0	25
	8	100	25
	8	200	25

RESULTS AND DISCUSSION

Experiments at the inlet condition (12 MPa, 80^{o}C)

Figure 2 shows the variations of corrosion rate and corrosion potential with time under different H_2S concentrations. Without H_2S, the corrosion rate is about 90 mm/y at the beginning of the experiment. Note that the corrosion rate decreased after 15 hours because of the change in solution chemistry within the autoclave caused by release of ferrous ion (Fe^{2+}) and the formation of protective iron

carbonate ($FeCO_3$), which is an experimental artifact and would not happen in the field conditions. With the presence of 100 ppm of H_2S, the initial corrosion rate was much lower than in the pure CO_2 condition, and the corrosion rate and corrosion potential were constant with time. This indicates that addition of small amount of H_2S reduced the corrosion rate almost 10 times under high pressure conditions. With 200 ppm of H_2S, the corrosion rate also starts out initially with similar values as for the case with 100 ppm H_2S, and then decreased to a low value, in the range of 1 ~ 2 mm/y.

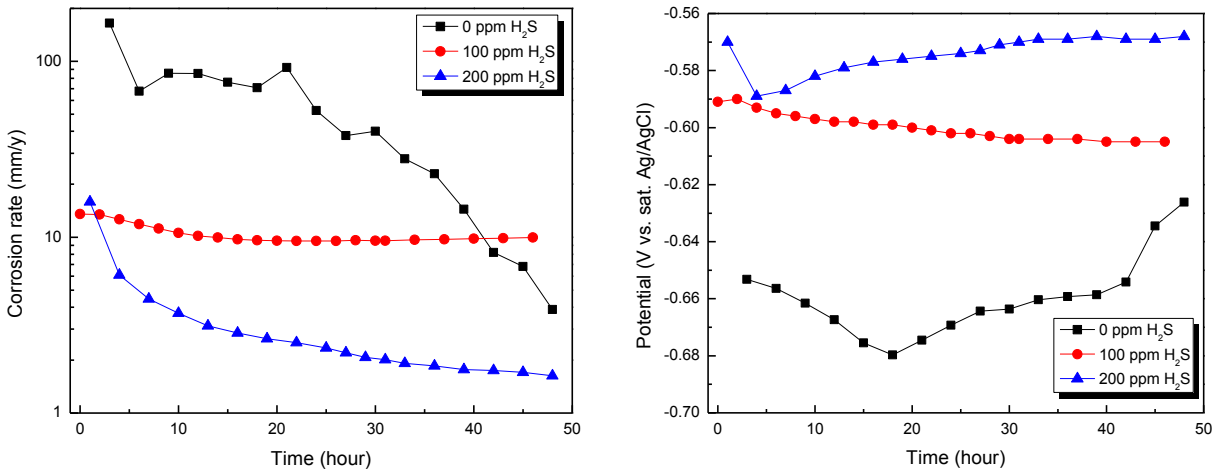

(a) (b)

Figure 2: LPR data of CS in CO_2 saturated brine containing 0, 100 and 200 ppm H_2S at 12 MPa CO_2 and 80°C: (a) Corrosion rate, (b) Corrosion potential.

Figure 3 shows the surface and cross-section SEM images of the corroded samples after 2 days at 12 MPa CO_2 and 80°C with different H_2S concentrations. In the presence of 200 ppm H_2S, the corrosion product layer is more compact and adherent to the metal surface, providing better corrosion protection. Figure 4 shows the XRD pattern of the corrosion product layer formed at 12 MPa and 80°C with 200 ppm H_2S. The layer formed in this condition showed a combination of FeS and $FeCO_3$. Therefore, the corrosion rate decrease in this case is because of the formation of a protective corrosion product layer on the surface.

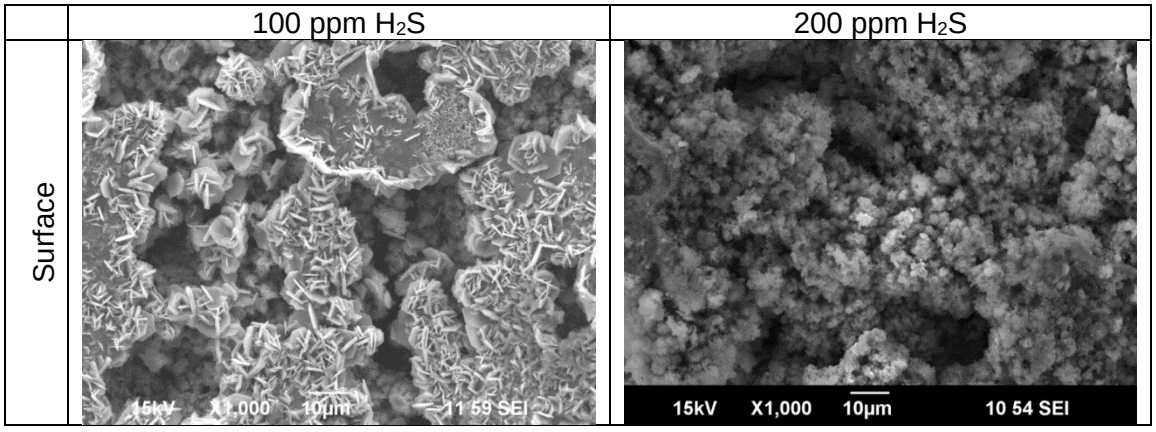

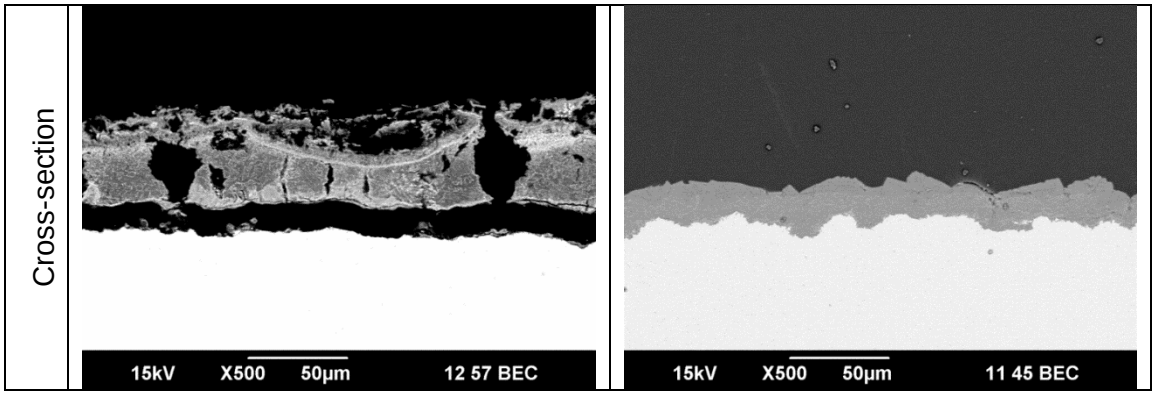

Figure 3: SEM surface and cross-sectional analyses of CS after corrosion experiment at 12 MPa CO_2 and 80°C with different H_2S concentrations.

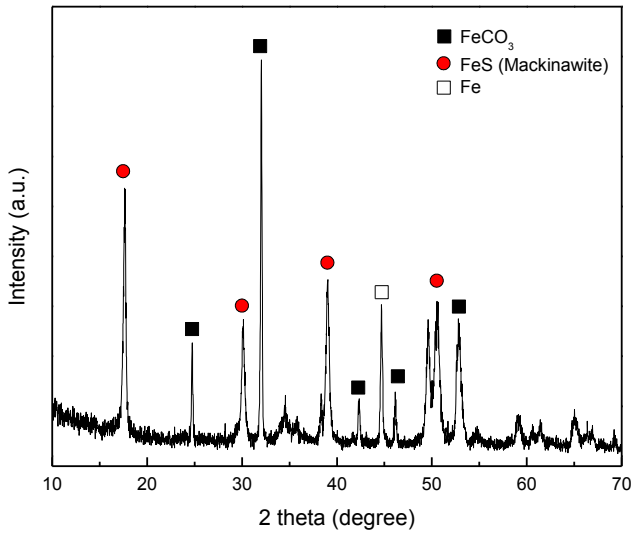

Figure 4: Result of XRD analysis for CS exposed to 12 MPa CO_2 and 80°C with 200 ppm H_2S.

Although the addition of H_2S provided a certain degree of protection to CS in the high pressure CO_2 condition, the corrosion rate was still high and it required additional protection in order to achieve the targeted inhibited corrosion rate (< 0.1 mm/y). Figure 5 shows LPR corrosion data of CS, 1Cr and 3Cr steels in the CO_2/H_2S system. It is interesting to note that CS shows the lowest corrosion rate in comparison with 1Cr and 3Cr steels. The 1Cr steel shows very active behavior in the CO_2/H_2S system with high corrosion rate and low corrosion potential. The result suggests that no beneficial effect of Cr is observed at these conditions (12 MPa CO_2 and 80°C) with 200 ppm H_2S, contrary to the case of pure CO_2 system.[16]

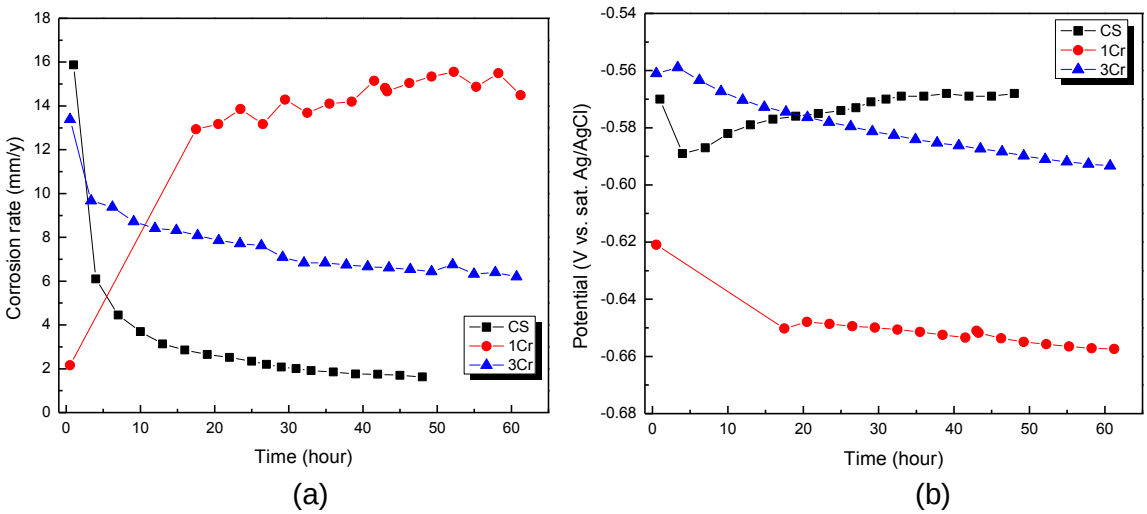

Figure 5: LPR data of different materials in CO_2 saturated brine containing 200 ppm H_2S at 12 MPa CO_2 and 80°C: (a) Corrosion rate, (b) Corrosion potential.

SEM and EDS surface analysis of specimens after corrosion experiments was conducted and the results are shown in Figure 6 and Table 3. CS formed a compact corrosion product layer, which is a combination of FeS and $FeCO_3$, and reduces the corrosion rate. However, 1Cr and 3Cr steels formed a Cr-rich layer on the surface (Table 3), which was identified as $Cr(OH)_3$.[21] It can be hypothesized that this layer reduces the adherence of the FeS layer to the metal surface, and, consequently compromises the corrosion resistance. Adherence of corrosion product layer to the metal surface is a key element in corrosion protectiveness of corrosion product layers. Furthermore, severe localized attack was observed on the surface of 1Cr steel.

	Before removing corrosion product	After removing corrosion product
CS	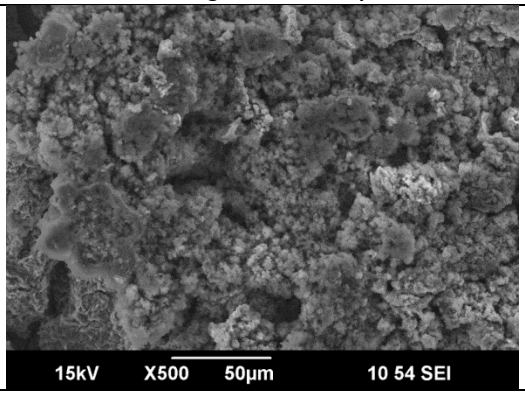	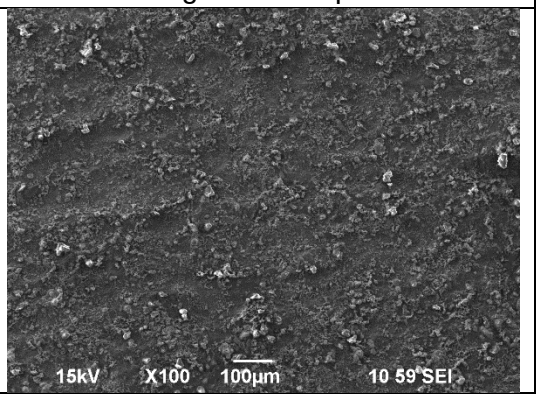

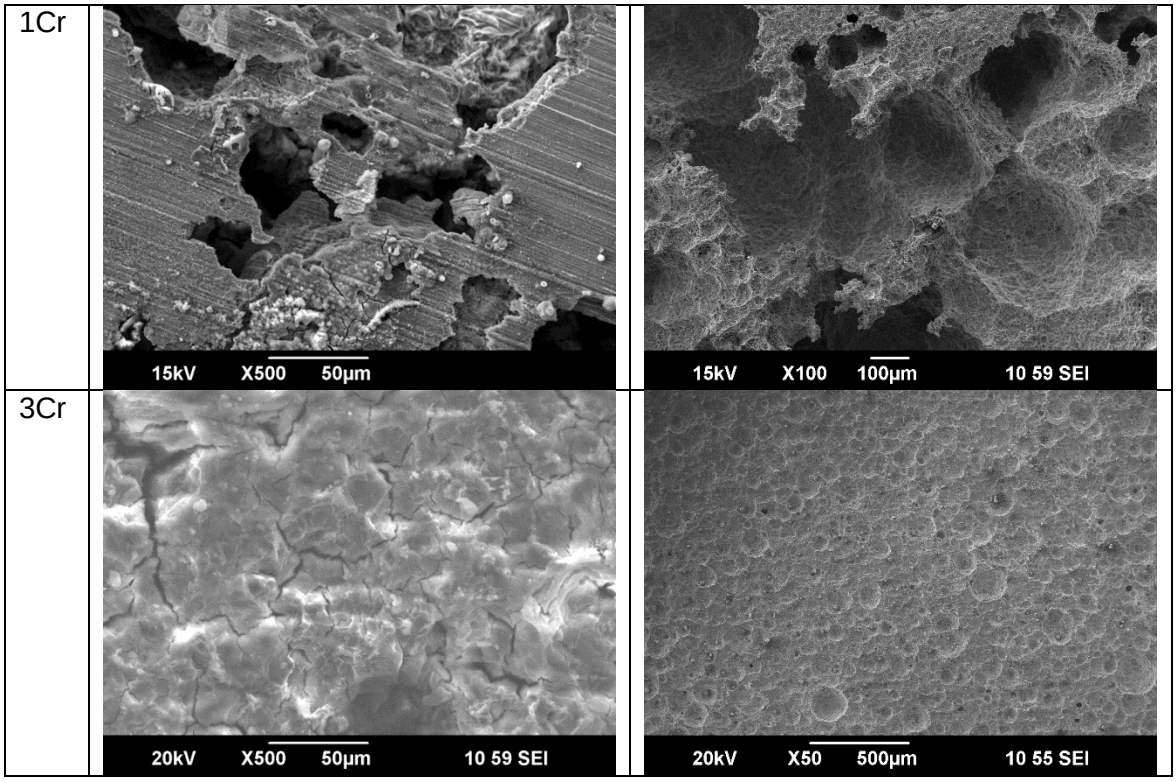

Figure 6: SEM surface analysis of different materials after corrosion experiments in NaCl electrolyte at 12 MPa CO_2 and 80°C with 200 ppm H_2S.

Table 3
EDS surface analysis of materials after corrosion experiment in brine system at 12 MPa CO_2 pressure containing 200 ppm H_2S and temperature of 80°C.

Element	CS (at.%)	1Cr (at.%)	3Cr (at.%)
C	28	37	20
O	39	6	27
S	6	3	10
Fe	22	53	7
Cr	0	36	36

Corrosion inhibitor (CI) were added to reduce the corrosion rate of CS in high pressure CO_2 with H_2S. Corrosion behavior of CS with different CIs in the CO_2/H_2S environment (12 MPa, 80°C, 200 ppm H_2S) is shown in Figure 7. The concentration of the CIs was fixed at 400 ppm based on the result of previous study in the pure CO_2 environments.[17] Although both CIs showed similar inhibition performance at the beginning of the test, only CI2 reduced the corrosion rate to lower than 0.1 mm/y at the end of the test.

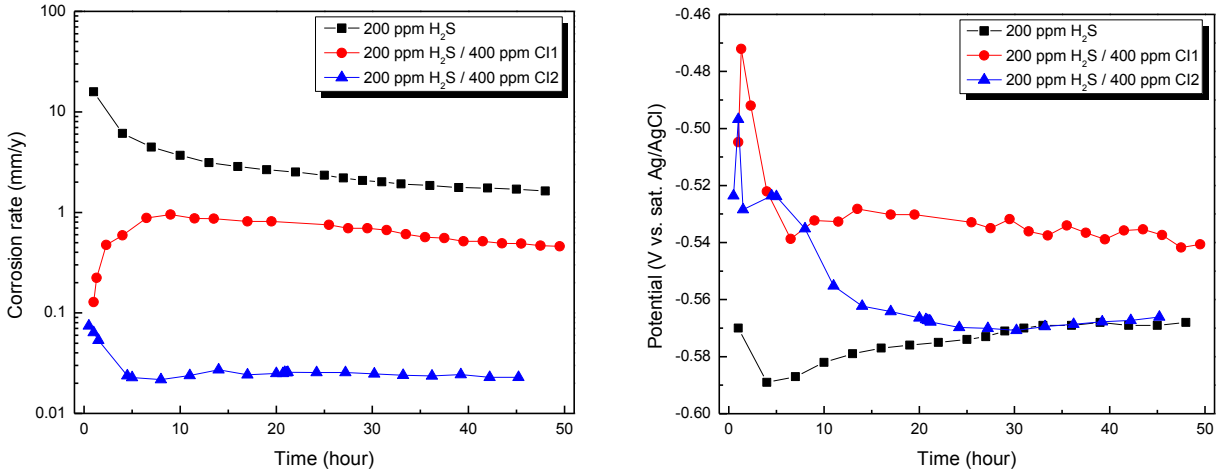

(a) (b)

Figure 7: LPR data of CS in CO_2 saturated brine with and without CIs at 12 MPa CO_2 and 80ºC (200 ppm H_2S): (a) Corrosion rate, (b) Corrosion potential.

According to the surface analysis, Figure 8, a significant amount of corrosion products were found on the sample with CI1 whereas no visible corrosion attack was observed on the surface with CI2. In the presence of CI1, the corrosion products contain high amounts of sulfur (S) (Table 4). This can be postulated to be due to formation of elemental S resulting from the reaction between thiosulfate and H_2S, as described by Siu and Jia:[22]

$$S_2O_3^{2-} + 2H_2S + 2H^+ \rightarrow 4S + 3H_2O \quad (1)$$

This formation of elemental S could be a reason for insufficient inhibition with CI1.

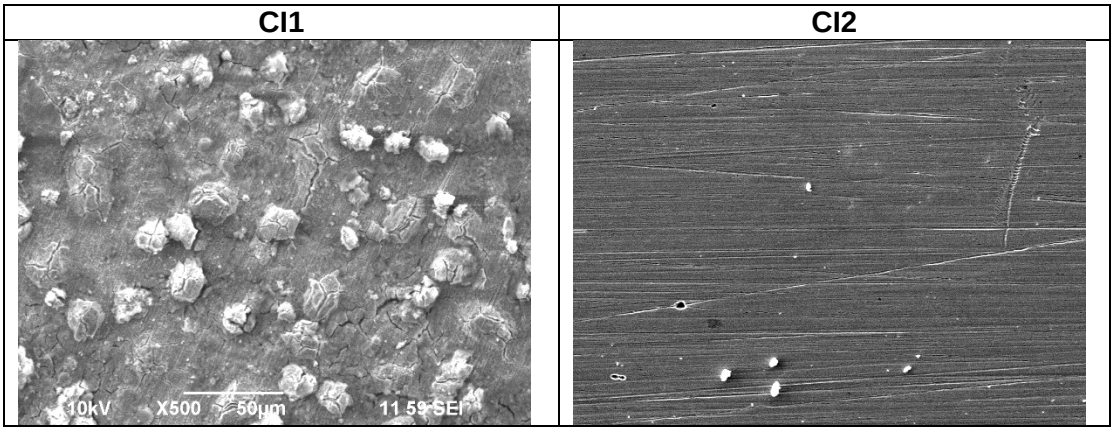

Figure 8: SEM images of the sample surface in CO_2 saturated 1 wt.% NaCl solution with the presence of 400 ppm of inhibitors at 12 MPa and 80ºC (200 ppm H_2S): (a) CI1, (b) CI2.

Table 4
EDS surface analysis of the sample after corrosion experiments with CI1 and CI2 at 12 MPa CO_2 and 80ºC (200 ppm H_2S).

Element	CI1 (at.%)	CI2 (at.%)
C	52	18
O	11	2
S	11	1
Fe	20	79

Experiments at the outlet condition (8 MPa, 25ºC)

Corrosion rates and corrosion potentials of CS at 8 MPa and 25ºC in CO_2 saturated 1 wt.% NaCl electrolyte with the presence of 0, 100, and 200 ppm of H_2S are shown in Figure 9. Without H_2S, the corrosion rate is constant about 10 mm/y from the beginning to the end of the experiment. With the presence of H_2S, again the corrosion rate was lower than the pure CO_2 condition. Although the corrosion rate with 200 ppm H_2S starts at a lower value than the case with 100 ppm H_2S, the corrosion rates for both conditions show similar values of around 0.3 mm/y after 15 h.

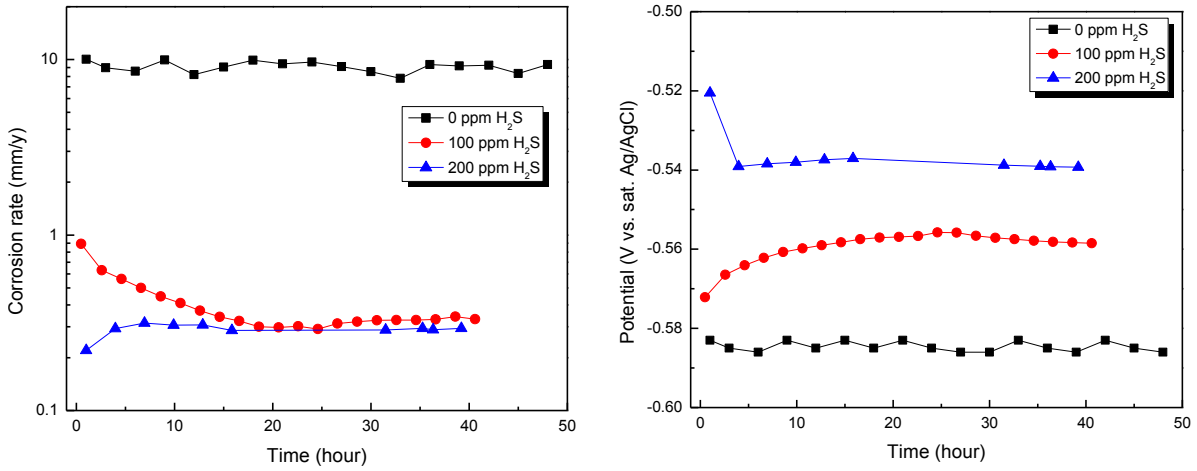

(a) (b)

Figure 9: LPR data of CS in CO_2 saturated brine containing 0, 100 and 200 ppm H_2S at 8 MPa CO_2 and 25ºC: (a) Corrosion rate, (b) Corrosion potential.

SEM surface and cross-section analysis for the effect of H_2S at 8 MPa and 25ºC is shown in Figure 10. CS is unable to form a $FeCO_3$ corrosion product layer at 25ºC. Therefore, the absence of this $FeCO_3$ at 25ºC means there is no as protectiveness due to corrosion product layer formation, as occurred at the inlet condition (12 MPa and 80ºC). In the system without H_2S, there was only a small amount of iron carbide (Fe_3C) on the surface; this is a residue of cementite in the steel when corrosion dissolved the ferrite phase. With 200 ppm H_2S, the surface was covered by a thin but more adherent S-containing corrosion product, which provides corrosion protection.

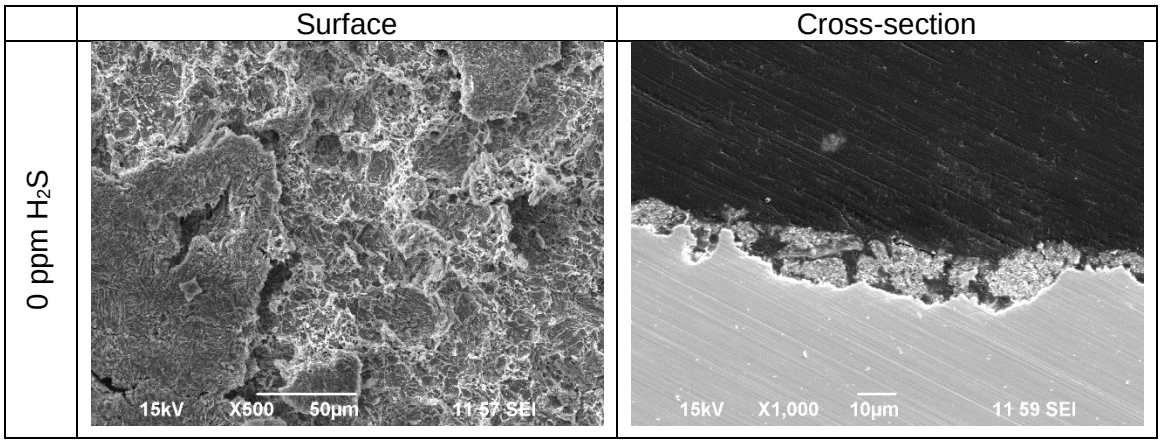

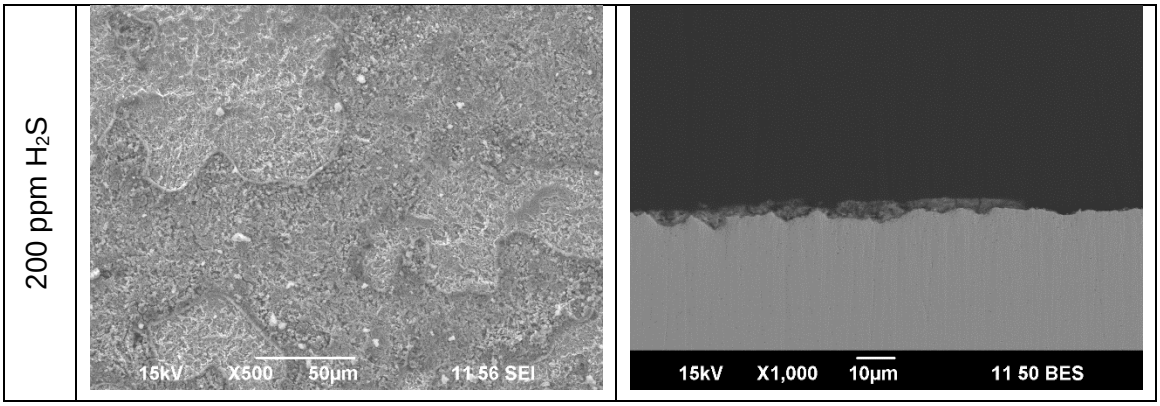

Figure 10: SEM and EDS surface analysis of CS after corrosion experiment at 8 MPa CO_2 and 25°C with different H_2S concentrations.

Figure 11 shows LPR corrosion data of CS and 3Cr steel in the 1 wt.% NaCl electrolyte at 8 MPa CO_2 and 25°C with 200 ppm H_2S. CS showed lower corrosion rate from the very beginning of the experiment, which means that a protective FeS layer immediately formed on the surface. However, 3Cr steel showed a drop in corrosion rate after a few hours then reached a stable corrosion rate similar to CS. The LPR results suggest that at the outlet condition, 3Cr steel shows a comparable corrosion performance with CS in a CO_2/H_2S system.

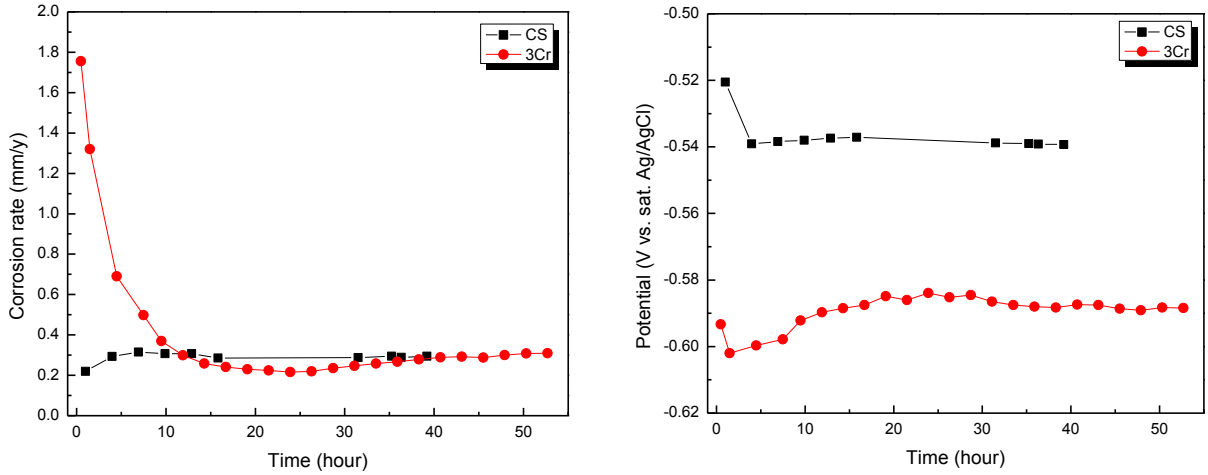

(a) (b)

Figure 11: LPR data of different materials in CO_2 saturated brine containing 200 ppm H_2S at 8 MPa CO_2 and 25°C: (a) Corrosion rate, (b) Corrosion potential.

Figure 12 shows SEM surface analysis of CS and 3Cr steel after removing corrosion product using Clarke's solution (20 g antimony trioxide, 50 g stannous chloride and hydrochloric acid to make 1,000 mL). In the case of CS, SEM surface analysis shows uniform corrosion attack on the surface. However, it shows localized corrosion of 3Cr steel occurs. High resolution optical profilometry was used to study the depth of the surface features associated with the observed localized corrosion attack.

Figure 13 shows the results of high resolution optical profilometry analysis of several pits observed on the cleaned 3Cr steel exposed to 8MPa CO_2 and 25°C with 200 ppm H_2S. According to the depth of the deepest pits, the maximum localized corrosion rate was measured to be 8 mm/y, which is 26 times higher than the general corrosion rate.

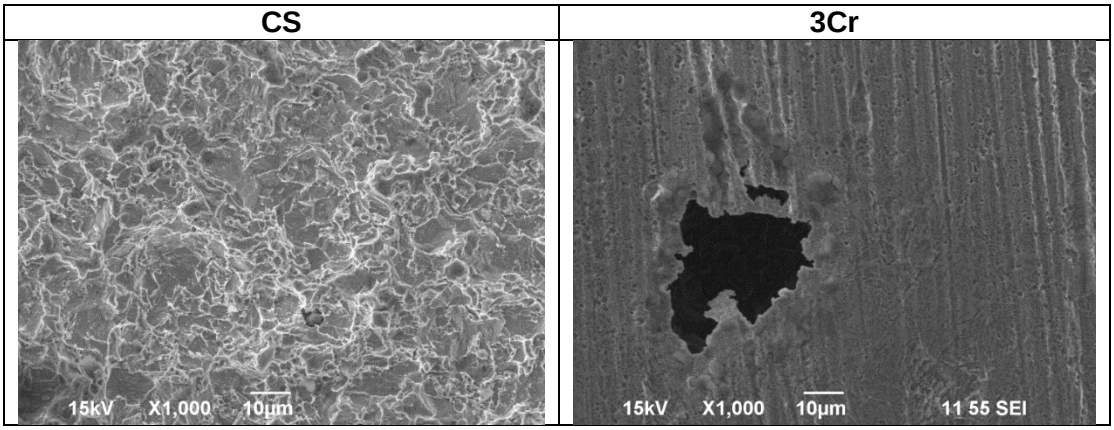

Figure 12: SEM images of CS and 3Cr steel after removing corrosion products.

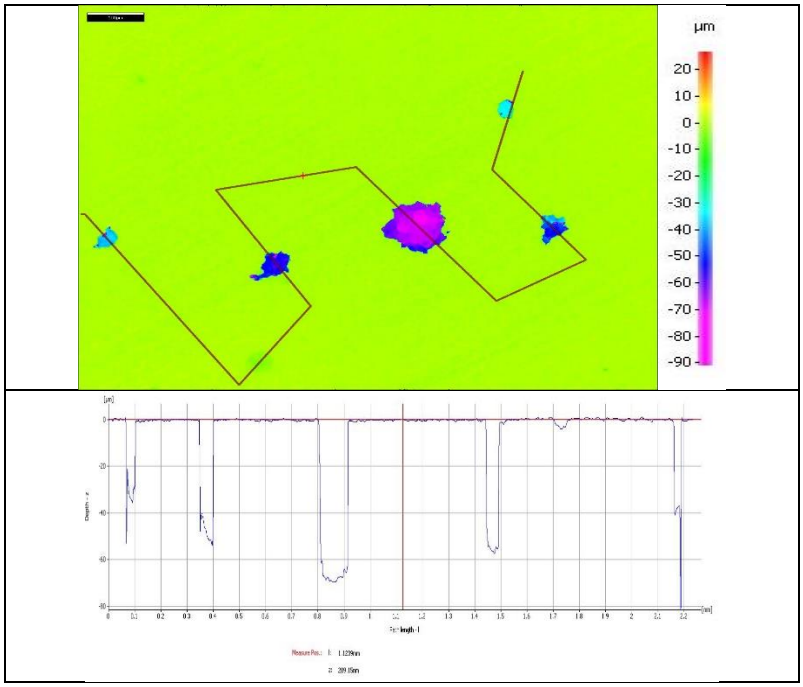

Figure 13: Surface analysis of 3Cr steel after corrosion experiment in brine system at 80 bar CO_2 pressure containing 200 ppm H_2S and temperature of 25°C.

The corrosion rate and corrosion potential of CS as a function of time with and without H_2S and CI2 in the outlet condition are shown in Figure 14. The addition of 200 ppm of H_2S decreased corrosion rate significantly from about 10 mm/y to about 0.3 mm/y, and the addition of CI2 in the CO_2/H_2S environment decreased the corrosion rate to much lower values (less than 0.1 mm/y).

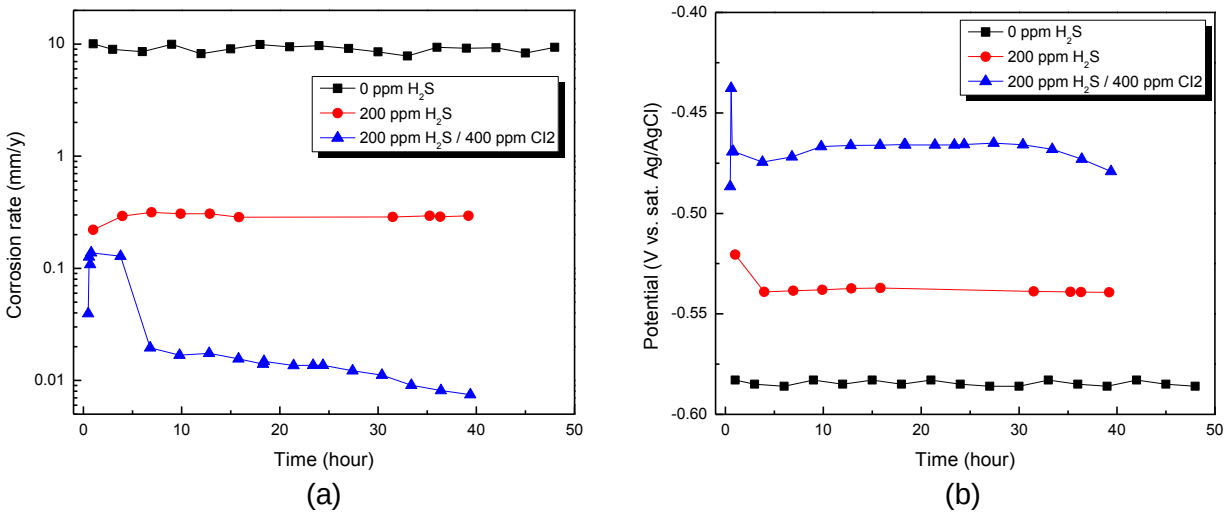

Figure 14: LPR data of CS in CO_2 saturated brine with and without H_2S and CI2 at 8 MPa CO_2 and 25°C: (a) Corrosion rate, (b) Corrosion potential.

SEM surface analysis of the sample surface before and after removing corrosion products once again confirms the superior inhibition performance of CI2 in the outlet condition (Figure 15).

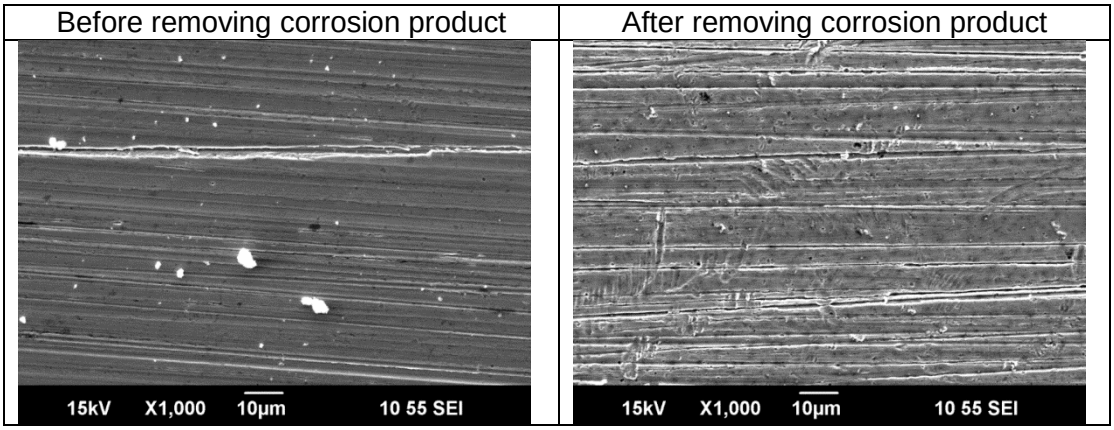

Figure 15: SEM images of the sample surface in CO_2 saturated 1 wt.% NaCl solution with the presence of 400 ppm of CI2 at 8 MPa CO_2 and 25°C with 200 ppm H_2S.

CONCLUSIONS

The corrosion mechanisms and corrosion protection of CS in a CO_2/H_2S system at different conditions were investigated by conducting electrochemical measurements and using surface analytical techniques. The following conclusions are drawn:

- The presence of small amounts of H_2S reduces the corrosion rate of CS in high pressure CO_2 conditions.
- The corrosion resistance of low Cr steels was worse than that of CS in high pressure CO_2 condition with some H_2S, indicating that applications of low Cr steels are limited to pure CO_2 condition.
- Adding 400 ppm of imidazoline-type corrosion inhibitor can be utilized in order to reduce the corrosion rate of CS below 0.1 mm/y in high pressure CO_2 conditions with some H_2S.

REFERENCES

1. S. Sim, I. S. Cole, Y.S. Choi, N. Birbilis, “A Review of the Protection Strategies against Internal Corrosion for the Safe Transport of Supercritical CO_2 via Steel Pipelines for CCS Purposes,” *International Journal of Greenhouse Gas Control* 29 (2014): p. 185.
2. L. Wei, Y. Zhang, X. Pang, K. Gao, “Corrosion Behaviors of Steels under Supercritical CO_2 Conditions,” *Corrosion Reviews* 33 (2015): p. 151.
3. S. Sarrade, D. Feron, F. Rouillard, S. Perrin, R. Robin, J.C. Ruiz, H.A. Turc, “Overview on Corrosion in Supercritical Fluids,” *Journal of Supercritical Fluids* 120 (2017): p. 335.
4. Y. Xiang, M. Xu, Y.S. Choi, “State-of-the-Art Overview of Pipeline Steel Corrosion in Impure Dense CO_2 for CCS Transportation: Mechanisms and Models,” *Corrosion Engineering, Science and Technology* 52 (2017): 485.
5. R. Barker, Y. Hua, A. Neville, “Internal Corrosion of Carbon Steel Pipelines for Dense-Phase CO_2 Transport in Carbon Capture and Storage (CCS) - A Review,” *International Materials Reviews* 62 (2017): p. 1.
6. Y. Zhang, X. Pang, S. Qu, X. Li, K. Gao, “Discussion of the CO_2 Corrosion Mechanism Between Low Partial Pressure and Supercritical Condition,” *Corrosion Science* 59 (2012): p. 186.
7. M. Seiersten, K.O. Kongshaug, “Materials Selection for Capture, Compression, Transport and Injection of CO_2”, in Carbon Dioxide Capture for Storage in Deep Geologic Formations, Vol. 2, D.C. Thomas and S.M. Benson Eds. (Elsevier Ltd. 2005), pp. 937
8. Y.S. Choi, S. Nesic, D. Young, “Effect of Impurities on the Corrosion Behavior of CO_2 Transmission Pipeline Steel in Supercritical CO_2-Water Environments,” *Environmental Science and Technology* 44 (2010): p. 9233.
9. Y.S. Choi, S. Nesic, “Determining the Corrosive Potential of CO_2 Transport Pipeline in High pCO_2–Water Environments,” *International Journal of Greenhouse Gas Control 5* (2011): p. 788.
10. M.F. Mohamed, A.M. Nor, M.F. Suhor, M. Singer, Y.S. Choi, S. Nesic, "Water Chemistry for Corrosion Prediction in High-pressure CO_2 Environments," CORROSION 2011, paper no. 11375 (Houston, TX: NACE, 2011).
11. A.M. Nor, M.F. Suhor, M.F. Mohamed, M. Singer, S. Nesic, "Corrosion of Carbon Steel in High CO_2 Environment: Flow Effect," CORROSION 2011*,* paper no. 11245 (Houston, TX: NACE, 2011).
12. Y. Zhang, X. Pang, S. Qu, X. Li, K. Gao, “The Relationship Between Fracture Toughness of CO_2 Corrosion Scale and Corrosion Rate of X65 Pipeline Steel Under Supercritical CO_2 Condition,” *International Journal of Greenhouse Gas Control* 5 (2011): p. 1643.
13. A.M. Nor, M.F. Suhor, M.F. Mohamed, M. Singer, S. Nesic, “Corrosion of Carbon Steel in High CO_2 Containing Environments: the Effect of High Flow Rate,” CORROSION 2012, paper no. 0001683 (Houston, TX: NACE, 2012).
14. Y.S. Choi, D. Young, S. Nesic, L.G.S. Gray, “Wellbore Integrity and Corrosion of Carbon Steel in CO_2 Geologic Storage Environments: A Literature Review,” *International Journal of Greenhouse Gas Control* 16S (2013): p. S70.
15. M.F. Mohamed, “Water Chemistry and Corrosion Inhibition in High Pressure CO_2 Corrosion of Mild Steel,” Master thesis, (Ohio University, 2015).
16. Y.S. Choi, S. Hassani, T.N. Vu, S. Nesic, A.Z.B. Abas, A.M. Nor, M.F. Suhor, “Corrosion Inhibition of Pipeline Steels under Supercritical CO_2 Environment,” CORROSION 2017, paper no. 9153 (Houston, TX: NACE, 2017).
17. Y.S. Choi, S. Hassani, T.N. Vu, S. Nesic, A.Z.B. Abas, “Effect of H_2S on the Corrosion Behavior of Pipeline Steels in Supercritical and Liquid CO_2 Environments,” *Corrosion* 72 (2016): 999.
18. L. Wei, X. Pang, K. Gao, “Effect of Small Amount of H_2S on the Corrosion Behavior of Carbon Steel in the Dynamic Supercritical CO_2 Environments,” *Corrosion Science* 103 (2016): 132.
19. L. Wei, X. Pang, K. Gao, “Corrosion of Low Alloy Steel and Stainless Steel in Supercritical $CO_2/H_2O/H_2S$ Systems,” *Corrosion Science* 111 (2016): 637.
20. Z. Liua, X. Gao, L. Dua, J. Lia, P. Li, C. Yu, R.D.K. Misra, Y. Wang, “Comparison of Corrosion Behaviour of Low-Alloy Pipeline Steel Exposed to H_2S/CO_2-Saturated Brine and Vapour-Saturated H_2S/CO_2 environments,” *Electrochimica Acta* 232 (2017): 528.

21. S. Hassani, T.N. Vu, N.R. Rosli, S.N. Esmaeely, Y.S. Choi, D. Young, S. Nesic, “Wellbore Integrity and Corrosion of Low Alloy and Stainless Seels in High pressure CO_2 Geologic Storage Environments: An Experimental Study,” *International Journal of Greenhouse Gas Control* 23 (2014): p. 30.
22. T. Siu, C.Q. Jia, “Kinetics of Reaction of Sulfide with Thiosulfate in Aqueous Solution,” *Industrial & Engineering Chemistry Research* 38 (1999): p. 1306.